MAUSAM, **72**, 1 (January 2021), 187-198

551.515.2 (267.37 : 267.64)

Understanding differences in tropical cyclone activity over the Arabian Sea and Bay of Bengal

IRIS C. LIU, SUZANA J. CAMARGO* and ADAM H. SOBEL**

Department of Physics and Astronomy, Barnard College, Columbia University, New York

**Lamont-Doherty Earth Observatory, Columbia University, Palisades, New York*

***Department of Applied Physics and Applied Mathematics and*

Department of Earth and Environmental Sciences, Columbia University, New York

e mail : ahs129@columbia.edu

सार – उत्तर हिंद महासागर के बेसिन के भीतर, बंगाल की खाड़ी (BoB) में उष्णकटिबंधीय चक्रवात (TC) की सक्रियता अरब सागर (AS) की तुलना में काफी अधिक है। लेखकों ने दोनों बेसिनों के बीच इस अंतर के कारणों को समझने के लिए विशिष्ट पर्यावरणीय कारकों की भूमिकाओं का पता लगाने का प्रयास किया है। बेसिन में चक्रवात की उत्पत्ति और तूफान की तीव्रता के तत्काल समय और स्थानों पर पर्यावरणीय परिवर्तनों को सम्पूर्ण रूप में माना गया है। उप-बेसिनों के बीच पर्यावरणीय परिवर्ती में महत्वपूर्ण अंतर का पता लगाने के लिए दोनों उप-बेसिन के परिणामों की तुलना की गई है। उष्णकटिबंधीय चक्रवात उत्पत्ति सूचकांक (TCGI) की जांच यह निर्धारित करने के लिए भी की जाती है कि क्या इस सूचकांक का उपयोग करके पर्यावरण के संदर्भ में अरब सागर- बंगाल की खाड़ी के अंतर को समझाया जा सकता है। हालाँकि दोनों में सूचकांक द्वारा एक या दो कारकों में सक्रियता का समग्र स्तर अनुमानित है, लेकिन उन बेसिनों के बीच सूचकांक एक सापेक्षिक अंतर दर्शाता है जो प्रेक्षणों में लगभग सुसंगत हैं। उस आंशिक सफलता के आधार पर, अरब सागर- बंगाल की खाड़ी के अंतर में सबसे महत्वपूर्ण कारकों को शामिल करने वाले जलवायु विज्ञान के सूचकांक निर्धारित करने के लिए यह जांच की जाती है। कॉलम सापेक्ष आर्द्रता और ऊर्ध्वाधर पवन अपरूपण सबसे संभावित कारकों के रूप में हैं। परीक्षण से पता चलता है कि कॉलम सापेक्ष आर्द्रता सबसे महत्वपूर्ण कारक है, इस कारण अरब सागर पर अपेक्षाकृत शुष्क क्षोभ मंडल होने के कारण यहाँ मुख्य रूप से बंगाल की खाड़ी की तुलना में कम चक्रवात आते हैं।

ABSTRACT. Within the North Indian Ocean basin, tropical cyclone (TC) activity over the Bay of Bengal (BoB) is substantially greater than over the Arabian Sea (AS). The authors attempt to quantify the roles of specific environmental factors in order to understand the reasons for this difference between the two basins. Environmental variables are considered in the basin as a whole and in the immediate times and places at which cyclogenesis and storm intensification occur. The results for the two sub-basins are compared to determine which environmental variables differed significantly between the sub-basins. A tropical cyclone genesis index (TCGI) is also examined to determine whether the AS-BoB difference can be explained in terms of the environment using this index. Though the overall level of activity in both is under-predicted by the index by about a factor of two, the index shows a relative difference between the basins that is approximately consistent with that in observations. Based on that partial success, climatologies of the individual factors that comprise the index are examined to determine which ones are most important in the AS-BoB difference. Column relative humidity and vertical wind shear emerge as the most likely candidates. A closer examination suggests that column relative humidity is the more important factor and thus that the AS has fewer cyclones than the BoB primarily because it has a drier lower troposphere.

Key words – Tropical Cyclone (TC), Joint Typhoon Warning Center (JTWC).

1. Introduction

The North Indian Ocean (NIO) basin exhibits less tropical cyclone (TC) activity than any other basin in which TCs occur with any regularity (Gray, 1968; Singh *et al*., 2016). Despite the relative infrequency of NIO TCs, however, the densely-populated regions that bound the NIO mean that the impacts of TC activity there can be very large (Sahoo and Bhaskaran, 2016). These impacts motivate us to study TC activity in the NIO. The NIO can be divided into two sub-basins, the Arabian Sea (AS) and the Bay of Bengal (BoB). Prior studies have noted the climatological difference in TC activity between BoB and AS [(Figs. 1(a-c) & 2(a&b)]. In many cases, studies

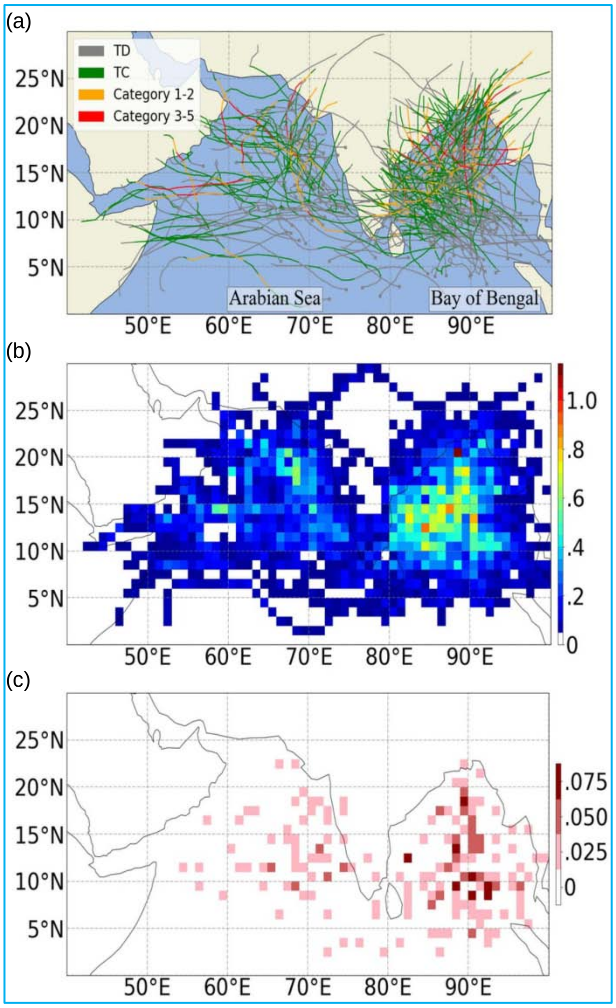

Figs. 1(a-c). TC tracks. (a) storm track density, (b) and first position density and (c) in the NIO (JTWC) for the period 1979-2018

focused in each sub-basin individually and explored which environmental conditions or large-scale modes of climate variability may control the TC activity occurring in each sub-basin.

Unlike other global basins, the NIO has two active seasons each year, one before the onset of the monsoon (the pre-monsoon season, from roughly April-June) and the other after the end of the monsoon (the post-monsoon season, from October-December) as described in Gray (1968). Li *et al.* (2019) analyzed which environmental parameters affect TC formation during the pre-monsoon season over the BoB, finding that variations in low-level vorticity contribute to TC genesis over the BoB during the pre-monsoon season, by comparing a genesis potential parameter in the environments of depressions that underwent cyclogenesis *vs*. those of depressions that did not.

Evan and Camargo (2011) and Ng and Chan (2012) analyzed the climatology and interannual variability of AS storms. Evan and Camargo (2011) identified large-scale features associated with TC variability over the AS and examined the environmental conditions associated with interannual variability in TC activity during both TC seasons. A study of changes in a genesis potential index revealed that variations in mid-level moisture largely dictate long-term variations in genesis rates over the AS.

Sattar and Cheung (2019) recently analyzed the asymmetry between the AS and BoB, focusing on years in which either the AS or BoB experienced the majority of the TC activity in the NIO, in order to evaluate which environmental factors account for the asymmetry that occurs between years in which the AS develops substantially more storms *vs*. those in which the BoB does. Their results revealed that greater moisture was available over the AS during the years in which AS had greater TC activity.

Singh *et al.* (2019) hypothesized that higher sea surface temperature (SST) and higher moisture content available over the BoB make climatological TC activity greater over the BoB than over the AS. Similarly, Sahoo and Bhaskaran (2016) attributes the higher activity in the BoB to higher SST and the presence of disturbances from the Western North Pacific there. Recently, a comparison of the TC activity in the AS and BoB in different epochs using a genesis index was performed by Baburaj *et al.* (2020), while two regional dynamical models were used to compare TC activity in the two sub-basins in Vishnu *et al.* (2019).

In recent years, there has been considerable interest in regional trends of TC activity. Similarly to other regions, a few studies have explored these trends over the NIO [Sahoo and Bhaskaran (2016); Balaji *et al.* (2018); Singh *et al.* (2019)]. However, the robustness of these trends remains an issue, due to the brevity of the record with reliable data quality, as discussed in Singh *et al.* (2020), so that typically only data from the satellite era are considered robust (Kossin *et al.*, 2020). Most studies identify a decreasing trend in the total number of TCs in the NIO, but an increase in the occurrence of the most intense storms there. Interestingly, future TC projections of the TC activity [Murakami and Sugi (2012); Murakami *et al.* (2017); Bell *et al.* (2020)] are different between the two sub-basins, with an increase in TC activity in the AS and no change or a decrease in activity in the BoB. Therefore, it seems imperative to have a better understanding of the differences between the climatological characteristics of the two sub-basins in the present, in order to comprehend the reasons for this distinct behaviour in future TC activity over the NIO.

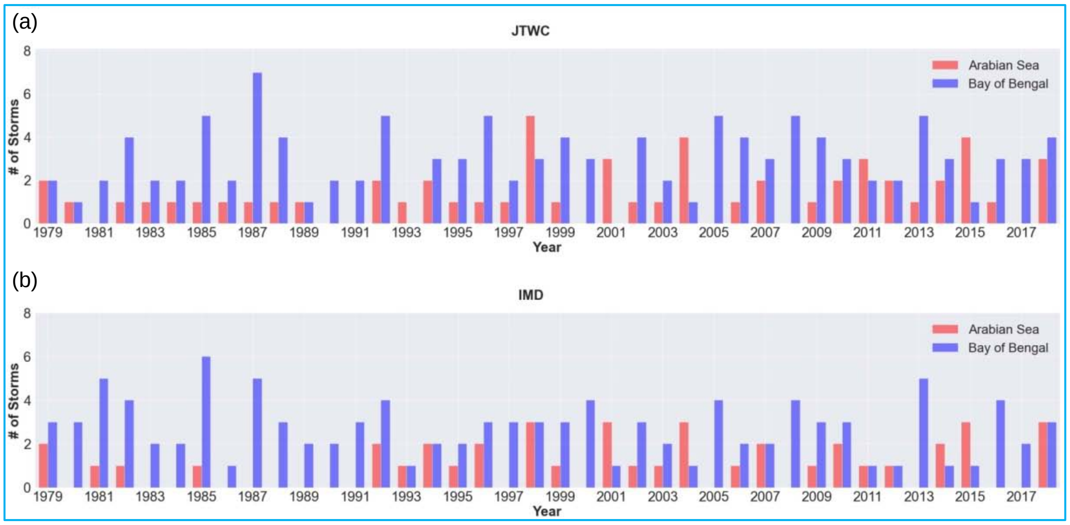

Figs. 2(a&b). Number of TCs in each sub-basin by year (1979-2018) for the JTWC. (a) and for IMD and (b) best-track data sets. Red bars denote Arabian Sea (AS) storms, blue bars Bay of Bengal (BoB) storms

While the studies discussed above yield insights about how specific environmental factors affect storm development in the AS and BoB, they do not explicitly assess the relative importance of the different environmental parameters to the asymmetry in TC activity between the AS and BoB on a climatological basis. In other words, why does the AS have fewer TCs than the BoB overall? The present study aims to address this question.

Section 2 outlines the methods and data sets used in the study. Section 3 details the results of our analysis and Section 4 describes the implications of these results.

2. Data and methodology

2.1. *Data*

The U. S. Joint Typhoon Warning Center (JTWC) best-track data set for the North Indian Ocean is used in our analysis (Chu *et al*., 2002). Storm location and maximum wind speed are available at 6-hour intervals starting in 1945, but we considered data for the period 1979 to 2018, as the best-track data from the satellite era are known to be more robust than those from before it (Schreck *et al*., 2014).

In addition to the JTWC data, the best-track data set from the India Meteorological Department (IMD) are used in Figs. 2(a&b) to compare the AS and BoB TC counts to those from JTWC. The IMD best-track data set starts in 1877, but only data from the period 1979 to 2018 were used in this study (IMD, 2011) corresponding to period analyzed in the best-track JTWC data set. Singh *et al*. (2020) showed that IMD data are robust in this period and considered to be in general agreement with the JTWC best-track data set.

Genesis is defined here as the first time at which the maximum wind speed of each TC is equal to or greater than 35 kt. We consider in our analysis the number of storms for the whole calendar year, as well as in the two NIO seasons : the pre-monsoon season defined as April to June (AMJ) and the post-monsoon season defined as October to December (OND).

The environmental fields used in our analysis are from the monthly ERA-Interim Reanalysis data set produced by the European Centre for Medium-Range Weather Forecasts (ECMWF) (Dee *et al*., 2011).

2.2. *Environmental parameters*

We consider a few large-scale environmental parameters of interest for the period 1979-2018, namely : sea surface temperature (SST), column relative humidity (CRH), potential intensity (PI), vertical wind shear (VSH) and the Tropical Cyclone Genesis Index (TCGI). SST was obtained directly from the ERA-Interim reanalysis, while the remaining four were computed as described below.

CRH is defined as the ratio of column-integrated water vapour path to saturation water vapour path and was calculated as outlined in Bretherton *et al*. (2004). The column-integrated water vapour W was obtained from the monthly ERA-Interim reanalysis over ocean grid points. The saturation water vapour path $W*$ was calculated from the temperature and surface pressure data at each pressure

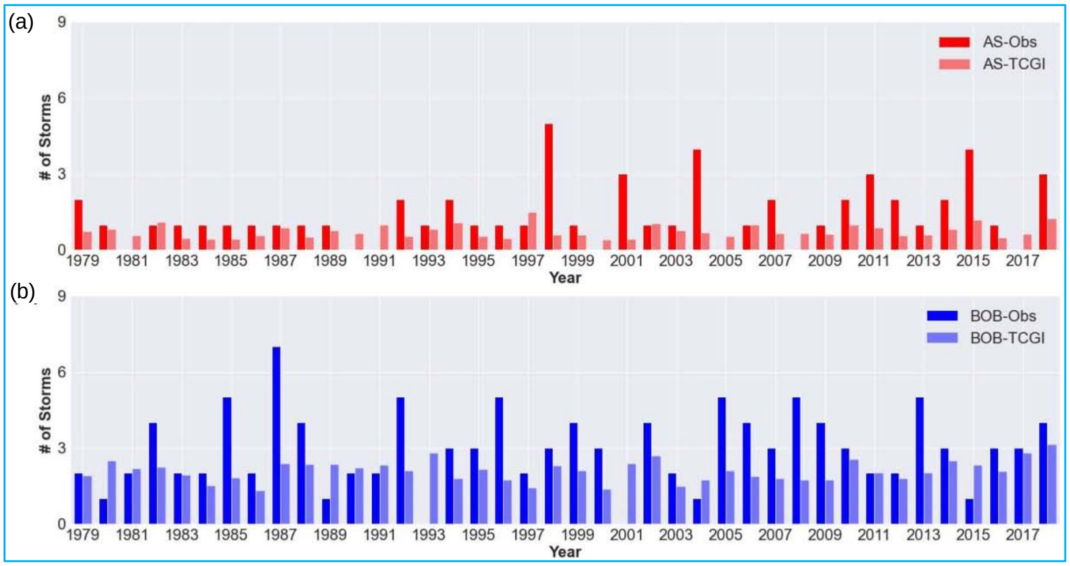

Figs. 3(a&b). Storm counts in observations (JTWC) and predicted by TCGI in each sub-basin by year (1979-2018). The top panel shows storm counts in the AS, the bottom panel in the BoB. Bright red (blue) and pale red (blue) correspond to observed and TCGI values in the AS (BoB), respectively

level and grid point, then vertically integrated. CRH is defined as the ratio W/W∗.

PI is the theoretical maximum intensity of a storm based on the thermodynamic state of the local atmosphere and ocean (Emanuel, 1988). PI is calculated from sea surface temperature (SST), sea level pressure and vertical profiles of atmospheric temperature and humidity following Bister and Emanuel (1998), with the modifications described in Bister and Emanuel (2002), taking into account dissipative heating.

VSH is defined as the magnitude of the difference in the magnitude of the monthly winds between the 850- and 200-hPa levels.

TCGI is a tropical cyclone genesis index obtained from a Poisson regression of observed genesis locations and environmental fields, which gives the probability of storm genesis globally, as described in Tippett *et al.* (2011). Here we used a version based on CRH, PI, absolute vorticity at 850 hPa and VSH, a modification of the original TCGI index presented in Camargo *et al.* (2014). By construction, the TCGI has units of TC number per time per area, so integrating over a region (*e.g.*, the BoB or AS) and over a time period gives the number of TCs that are predicted to occur based on the environmental parameters considered. These TCGI values can compared to the observed TC counts for each sub-basin and year, as shown in Figs. 3(a&b).

2.3. *Diagnostics*

To evaluate the magnitude of association between the observed and TCGI-predicted storm counts, Pearson *r* correlation coefficients were computed for the observed and predicted values for each sub-basin, within each active season.

Histograms containing environmental parameter values, computed from monthly data at the grid point closest to the TC center position at the time of genesis, were created to compare the distributions of the environmental parameters at TC formation across the BoB and AS. A non-parametric two-sided Mann-Whitney *U* test was then performed to evaluate whether or not the sub-basins exhibited statistically significant differences in any of the six parameters analyzed at the 95% confidence level (Mann and Whitney, 1947). This test was chosen because the environmental variables examined here were not found to be normally distributed and the storm samples for each sub-basin were too small to satisfy the conditions necessary for a parametric test for statistical significance.

In addition to the analyses described above at the time at of genesis (defined as the time at which the wind speed equals or exceeds 35 kt), the same analyses were also performed near each storm's first recorded position (at which wind speeds are generally less than 35 kt) and the location of storm lifetime maximum intensity (LMI,

TABLE 1

Number of tropical cyclones (NTC), cyclones in the categories 1-5 and 3-5 in the Saffir-Simpson Scale, named C15 and C35, respectively, as well TCGI averages for the AS, BoB and NIO for the full year and the pre-or post-monsoon seasons AMJ and OND. Also shown are the total of TCs that stay in the sub-basin that they formed and those that cross to the other sub-basin

	Year					
	AS		BoB		NIO	
Total NTC (%)	57 (29.08%)		139 (70.92%)		196 (100%)	
Total C15 (%)	8 (22.22%)		28 (77.78%)		36 (100%)	
Total C35 (%)	9 (33.33%)		18 (66.67%)		27 (100%)	
Mean NTC (STD)	1.43 (1.17)		3.48 (1.72)		4.90 (1.79)	
Mean TCGI (STD)	0.37 (0.13)		2.08 (0.42)		2.45 (0.49)	
	AMJ	OND	AMJ	OND	AMJ	OND
Mean NTC (STD)	0.30 (0.56)	0.70 (0.82)	0.73 (0.68)	1.90 (1.22)	1.03 (0.89)	2.60 (1.10)
Mean TCGI (STD)	0.31 (0.13)	0.42 (0.21)	0.75 (0.24)	1.33 (0.31)	1.06 (0.32)	1.75 (0.42)
	Stay	Cross	Stay	Cross	Stay	Cross
	56 (32.18%)	1 (4.55%)	118 (67.8%)	21 (95.45%)	174 (100%)	22 (100%)

defined as the highest recorded wind speed reached by the storm). The results were sufficiently similar to the results for genesis locations that they are not shown here.

3. Results

3.1. *TC activity in the NIO*

Fig. 1(a) shows the tracks of all NIO TCs in the period 1979-2018. Fig. 1(b) shows the track density over this period and Fig. 1(c) the genesis density. The greater activity in the BoB compared to the AS is evident in all three panels.

We are interested in differences between storm frequency in the BoB and AS, but must also address the complexity that some storms develop in one sub-basin and then migrate over the Indian sub-continent into the other sub-basin. Table 1 shows the relevant statistics. Out of the 196 TCs that formed in the basin over relevant time period 174 storms, or 88.78% of the total, remained within the sub-basin in which they formed. Of these 174 storms, 32.18% formed and remained in the AS while 67.82% formed and remained in the BoB. However, 22 storms, or 11.22%, crossed out of the sub-basin in which they formed and into the other. Of these 22, all but one - that is, 21 (95.45% of crossing TCs) - formed in the BoB and migrated into the AS, with the one exception forming in the AS and migrating into the BoB (4.55% crossing TCs).

If we consider the quantity of interest the frequency of genesis, then the BoB had 139 storms while the AS had 57 storms, yielding a climatological ratio of 2.4 BoB storms for every AS storm. If we consider instead the frequency of storm occurrence, the AS had 78 storms (now that those crossing from the BoB are included) while the BoB had 140, a ratio of 1.8. For the remainder of our study we will only consider the TC genesis frequency. Also shown in Table 1 are the number of TCs that reach category 1 (C15) and category 3 (C35) intensities in the Saffir-Simpson scale during their lifetime.

TABLE 2

Number of years in which the BoB had more and fewer storms than the AS and no storms in either sub-basins for the full year and the pre-or post-monsoon seasons AMJ and OND in both the JTWC and IMD best-track datasets

NTC	JTWC IMD Year	JTWC IMD AMJ	JTWC IMD OND
BoB > AS	30 29	17 13	22 29
BoB < AS	6 4	5 8	7 2
BoB = 0, AS ≠ 0	2 0	3 6	6 2
BoB ≠ 0, AS = 0	7 16	17 13	15 22

Figs. 2(a&b) show the number of storms that occurred in each sub-basin in each year during the period 1979-2018; the blue bar represents the number of TCs occurring over the BoB, while the red bar represents the number of storms occurring over the AS in the JTWC and IMD datasets. From the JTWC data, for 30 of the 40 years observed (75%), the BoB had a greater number of storms

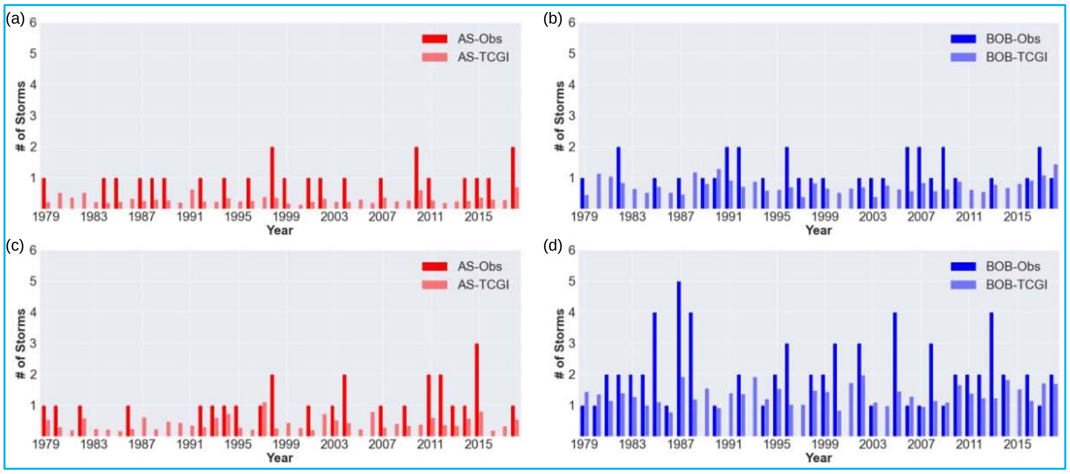

Figs. 4(a-d). TC counts in observations (JTWC) and predicted by integrating TCGI in each sub-basin by year and season (1979-2018). Bright red (blue) and pale red (blue) correspond to observed and TCGI values in the AS (BoB), respectively. Top panels are for AMJ and bottom panels 439 for OND)

than did the AS. In 1981, 1990, 1991, 2000, 2005, 2008 and 2017 all TC activity was concentrated in the BoB while the AS saw no storm development. By contrast, there were only two years (1993 and 2001) in which all storms occurred in the AS while there were none in the BoB (Table 2). Additionally, the BoB saw greater storm activity for 30 of the 40 years analyzed, while there were only six years in which the AS had more storms than the BoB (and four years in which both sub-basins had the same number of storms).

Best track data from the IMD yield similar findings over the same period. The BoB saw a greater frequency of storm formation for 29 of the 40 years analyzed, while the AS possessed a majority of the NIO's storm activity for only 4 years (2001, 2004, 2014 and 2015). Likewise, there were 16 years in which all storms formed over the BoB, while there were no years during which storms developed solely over the AS.

3.2. *Prediction of NIO TC activity with a genesis index*

As our goal is to understand the differences in TC activity between the AS and BoB in terms of differences in the large-scale environments, we next examine to what extent the TCGI, which quantifies our understanding of environmental control on TC genesis, is able to predict the observed rates of TC genesis in the two sub-basins of the NIO. Figs. 3(a&b) and 4(a-d) show time series of sub-basin observed and TCGI-predicted TC counts (the latter computed by integrating the TCGI over the sub-basin area, as described in Section 2) on a yearly and seasonal (pre-and post-monsoon TC seasons) basis, respectively.

As our primary interest is in explaining the climatological difference between the AS and BoB, we ask first whether the TCGI is able to predict that difference on a climatological, *i.e.*, time-averaged basis. The TCGI mean and percentage values are given in Table 1 for an easy comparison with the observed values. For the AS, the time mean annual totals are 1.40 storms for observed TCs and 0.73 storms for TCGI TCs, while for the BoB, the average number of TCs was 2.95 in the observations but 2.08 according to the TCGI. Thus the TCGI underestimates the observed genesis frequency by a factor of 1.4 in the BoB and 1.9 in the AS. While these are substantial errors, the TCGI does much better in predicting the relative difference between the sub-basins, predicting that the ratio of BoB to AS storms is 2.8 while the observed ratio is 2.1. We conclude that the TCGI, though biased low by about a factor of two in its absolute magnitude in the NIO, does better at predicting the relative TC genesis frequency difference between the sub-basins, over-predicting the BOB/AS ratio by 33%.

Figs. 4(a-d) provides a seasonal breakdown of the information in Figs. 3(a&b), in that the observed and TCGI-predicted TC counts are separated into pre-and post-monsoon seasons for each year. The time mean TC counts for storms occurring within the AS during the pre-monsoon season were 0.60 for the observed and 0.31 for the TCGI counts respectively, while for the post-monsoon season the time means were 0.68 and 0.42 for the observed and TCGI counts (Table 1). For the BoB, mean TC counts during the pre-monsoon season were 0.83 for the observed and 0.75 for the TCGI-integrated counts, while mean TC counts during the post-monsoon season were 1.78 for the observed and 1.33 for the TCGI (Table 1).

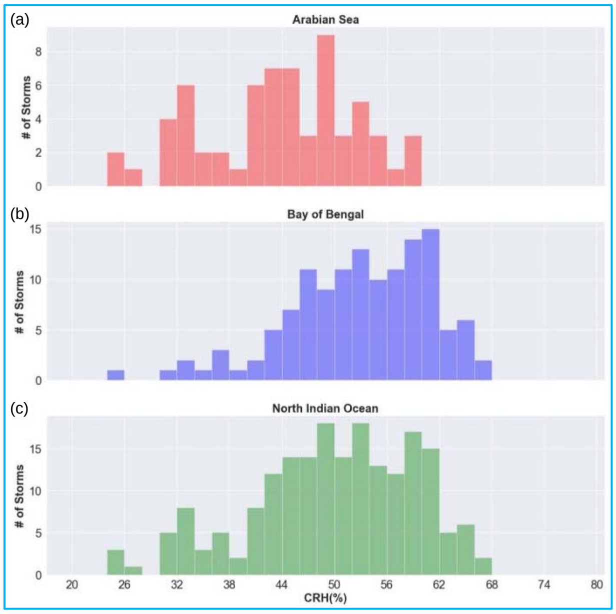

Figs. 5(a-c). Distributions of column relative humidity (CRH) near the TC genesis positions, red (a) for the Arabian Sea (AS), blue (b) for the Bay of Bengal and green (c) for the NIO basin

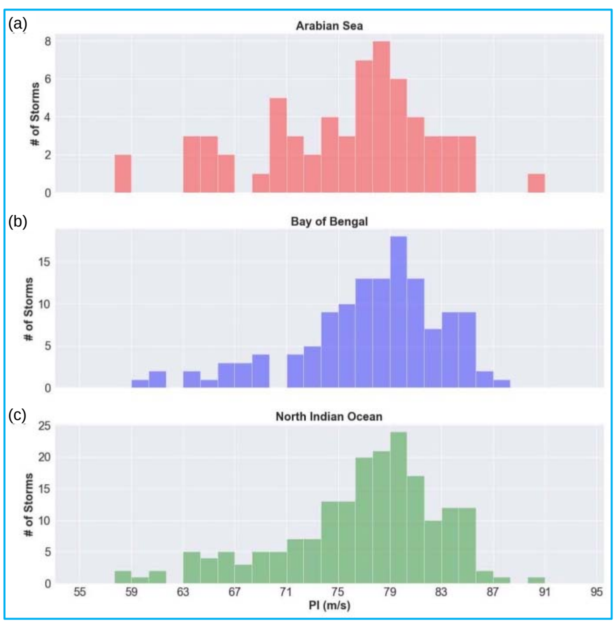

Figs. 6(a-c). Distributions of PI near the TC genesis positions, red (a) for the Arabian Sea (AS), blue (b) for the Bay of Bengal and green (c) for the NIO basin

Though the Pearson's *r* correlation values shown in Table 3 indicate seasonal correlation between the TCGI and observed counts to be low and not statistically significant, the above time means nonetheless show a reasonable degree of consistency between the TCGI and observations. We also note that, since the TCGI assumes

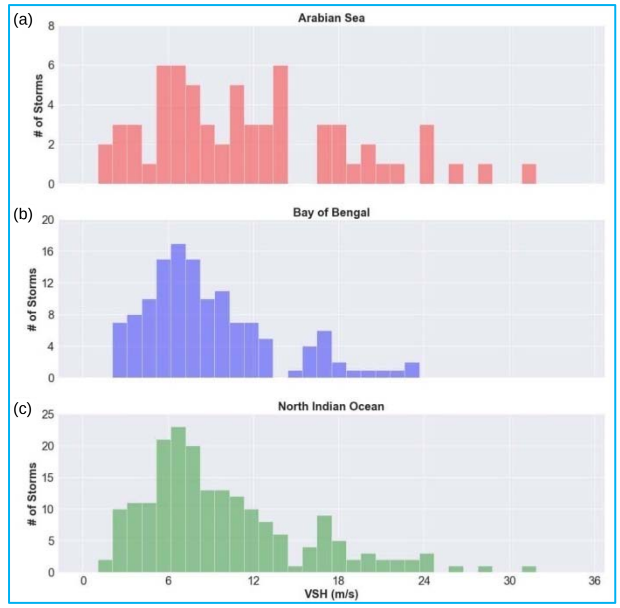

Figs. 7(a-c). Distributions of vertical shear (VSH) near the TC genesis positions, red (a) for the Arabian Sea (AS), blue (b) for the Bay of Bengal and green (c) for the NIO basin

TABLE 3

Correlations between the number of TCs and mean values of TCGI per year and per season (AMJ and SON) for the AS, BoB and NIO

	AS	BoB	NIO
AMJ	0.25	0.08	0.25
OND	0.29	0.04	-0.02
Year	0.20	-0.02	0.09

that genesis is a Poisson process, it is expected to perform better on larger samples. Thus, we should expect its predictions to be somewhat better for the annual climatology than for individual seasonal climatologies and much better for either of those than for individual years.

Given that the TCGI is able to explain at least some aspects of the BoB-AS difference in TC activity, we proceed to analyze individual variables that contribute to the TCGI, with the goal of determining their relative importance.

3.3. *TC environments at genesis*

We first examine histograms of individual variables at the TC genesis locations in Figs. 5-7(a-c). Histograms of CRH, PI and VSH values, respectively, are shown for the AS (red), BoB (blue) and entire NIO (green).

The CRH the histograms for the AS and BoB [Figs. 5(a-c)] are quite different. Both are bimodal, but the

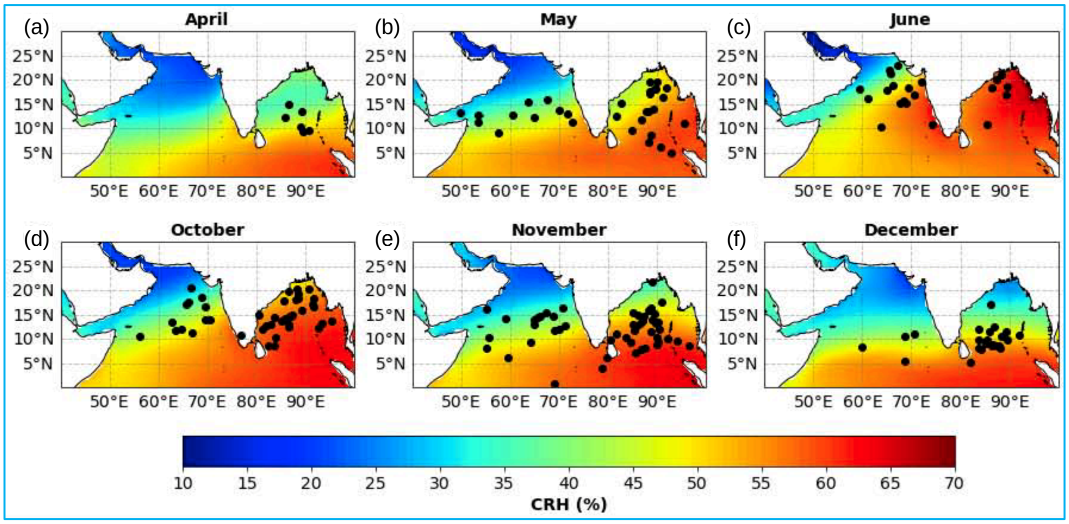

Figs. 8(a-f). TC genesis locations (black dots) column relative humidity (CRH) climatology (1981-2010) for different months. Top (bottom) row shows months of the pre-monsoon (post-monsoon) seasons

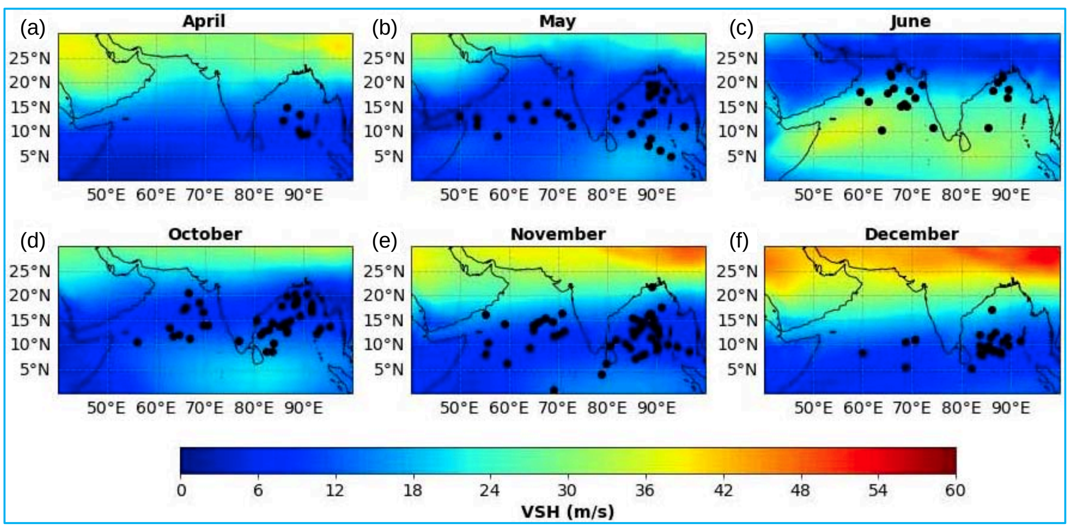

Figs. 9(a-f). TC genesis locations (black dots) vertical shear (VSH) climatology (1981-2010) for different months. Top (bottom) row shows months of the pre-monsoon (post-monsoon) seasons

AS one is more dramatically so; perhaps more importantly, the AS histogram is shifted to the left compared to the BoB one, indicating that AS TCs, on average, form at lower values of column relative humidity than do BoB TCs. The difference is highly significant according to the Mann-Whitney *U* test (*p*-value of 6.08×10^{-11}).

The histograms for PI [Figs. 6(a-c)], by contrast to those for CRH, are more similar between the AS and BoB; however, the difference between the two is still significant ($p = 0.03$) according to the Mann-Whitney *U* test.

Figs. 7(a-c) displays the AS and BoB VSH distributions. While the AS and BoB distributions both have peaks near 7 ms^{-1}, the AS histogram has considerably more mass at higher values, indicating that on average, AS storms form in conditions of higher shear than do BoB storms. The difference is significant per the Mann-Whitney *U* test ($p = 0.01$).

The results above indicate that TCs in the BoB and AS form in conditions of column relative humidity, potential intensity, vertical shear that are, on average, significantly different. The monthly 238 low-level absolute vorticity - the fourth variable used to construct the TCGI - shows very similar distributions, on the other hand (not shown). In the remainder of this section, we focus further on the CRH, PI and VSH fields, seeking

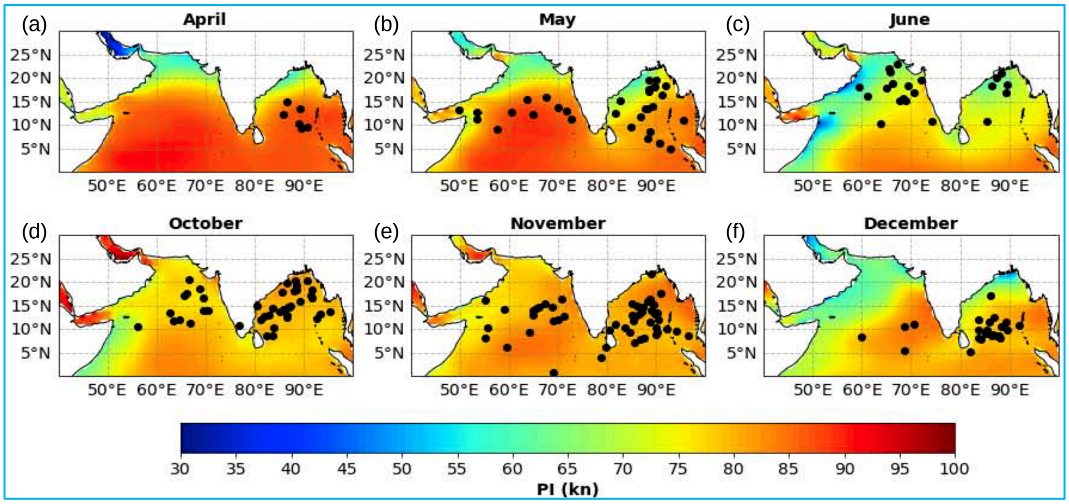

Figs. 10(a-f). TC genesis locations (magenta dots) potential intensity (PI) climatology (1981-2010) for different months. Top (bottom) row shows months of the pre-monsoon (post-monsoon) seasons

evidence as to whether one of those variables is more important than the others to the TC activity difference between the AS and BoB.

3.4. *Seasonal and spatial structure of climatological environmental fields*

Figs. 8(a-f) - 10(a-f) present spatial maps of the monthly CRH, VSH and PI climatologies, respectively. The black dots show the locations of each TC occurring in each respective month at its genesis location. These maps were constructed for each month in the pre-monsoon (AMJ) and post-monsoon (OND) seasons. From these figures we can see that the storms rarely form in conditions of either high climatological wind shear or low climatological column relative humidity. The most exceptions occur in the AS, where some storms form in the presence of relatively high shear in June and of relatively low humidity in October and November.

However, while a correspondence between storm genesis location and climatological CRH and VSH values are observed [Figs. 8(a-f) and 9(a-f)], we do not notice such a relation for PI and storm genesis location [Figs. 8(a-f)]. TC genesis does not particularly favour the locations or months in which PI is the highest, *e.g.*, quite a few storms form over relatively low PI in June, in both sub-basins and none form in April over the high PI in the AS. Overall, in fact, the BOB does not have consistently higher PI than does the AS, even though the PI at the times and places of genesis is on average slightly higher in the BOB than AS (as seen in the histograms above). Thus, we may infer that PI has less of an effect on TC genesis compared to CRH and VSH.

TABLE 4

RMS errors between seasonal (pre-and post-monsoon season) and yearly basin-integrated TC genesis events and TCGI for the AS, BoB and NIO

	AS	BoB	NIO
AMJ	0.61	0.76	0.97
OND	0.72	1.30	1.30
Year	1.34	1.58	1.69

Considering Figs. (8-10) further, we can see that the differences between the AS and BoB in CRH are more dramatic than those in VSH or PI. The AS is much drier than the BoB in the 260 entire pre-monsoon season, as well as in October and November - that is, two out of three months of the post-monsoon season, with the third (December) also showing a substantial difference in the more southern latitudes where most storms form during that month. The contrasts between the sub-basins in vertical shear are less dramatic than those in column relative humidity, while nearly 264 no contrast is observed between the sub-basins for PI. Interestingly, in June - the one month when climatological TC frequency in the AS exceeds that in the BoB - shear is actually greater in the AS [Fig. 9(c)]. Of course, since Figs. 8(a-f) and 9(a-f) show only the climatologies of CRH and VSH, they do not depict the actual environments at the specific times of storm formation. The histograms above, in Figs. 5(a-c) - 7(a-c), do capture the latter and show differences that are qualitatively consistent with those in Figs. 8(a-f) - 10(a-f)].

While Figs. 8(a-f) - 10(a-f) suggest that humidity is more important to the AS-BoB difference in TC frequency

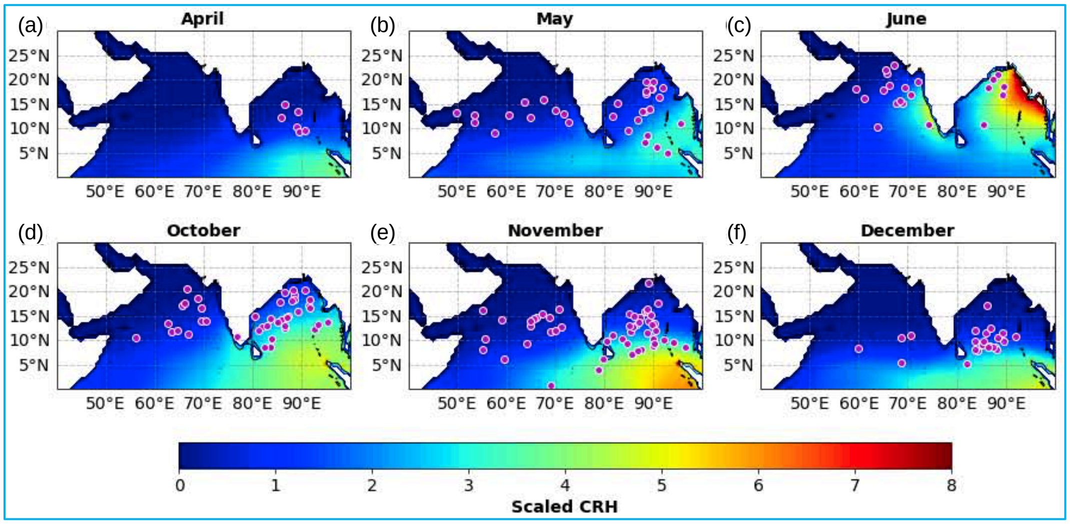

Figs. 11(a-f). TCGI-scaled climatological column relative humidity (CRH) values for different months. Top (bottom) row shows months of the pre-monsoon (post-monsoon) seasons. TC genesis locations given as magenta dots

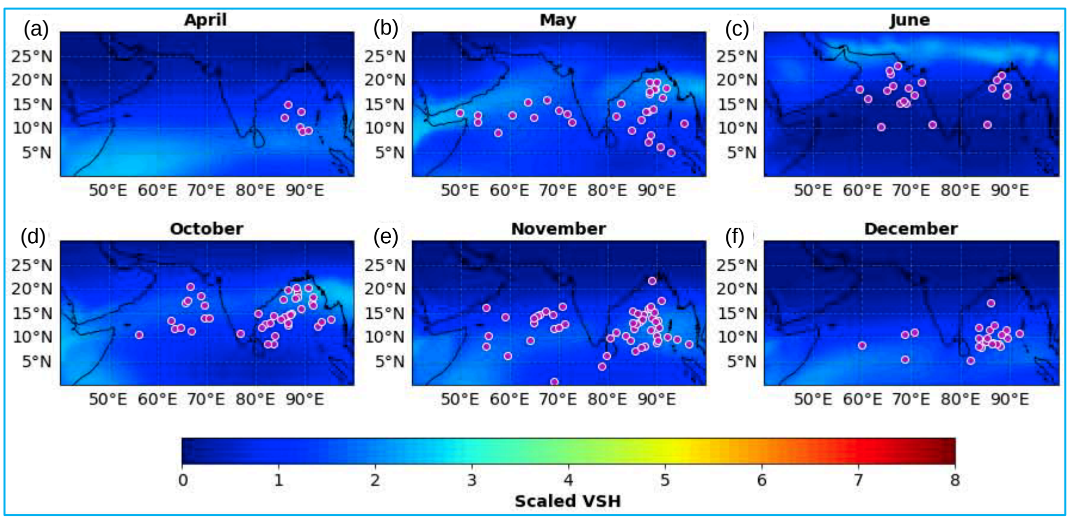

Figs. 12(a-f). TCGI-scaled climatological vertical shear (VSH) values for different months. Top (bottom) row shows months of the pre-monsoon (post-monsoon) seasons. TC genesis locations given as magenta dots

than either vertical shear or potential intensity, the TCGI allows us to quantify this difference further. The TCGI, being constructed by Poisson regression (Tippett *et al*., 2011) has the form $\mu = \Pi_i \exp(b_i X_i)$, where μ denotes the index itself, the X_i are individual environmental predictors and the bi are coefficients obtained from the regression; here i ranges from 1 to 5, with four environmental variables (PI, vertical shear, column relative humidity, low-level absolute vorticity) and one of the X_i set to unity to allow a constant term (intercept). By plotting the individual terms $\exp(b_i X_i)$, we can compare the relative importance of each term to the variations in the index as a whole and thus - to the extent that the index successfully predicts it - to the variations in actual TC frequency, where here our interest is in the AS-BoB difference. Figs. 11(a-f) - 13(a-f) show these for the CRH, VSH and PI, with storm genesis locations plotted as magenta points on top. Because the terms are multiplied rather than added to produce the TCGI, the absolute magnitudes should not be compared, but rather their relative variations, so each field is scaled by its total spatial variance. Months of the pre-monsoon season are given in the top row, while those of the post-monsoon are given in the bottom row. These figures reinforce the conclusion that the variations in humidity are more important than the variations in shear to the climatological AS-BoB difference in TC activity. The PI alone, in fact, would appear to favor the AS over the BOB slightly during April and May and is comparable in the other

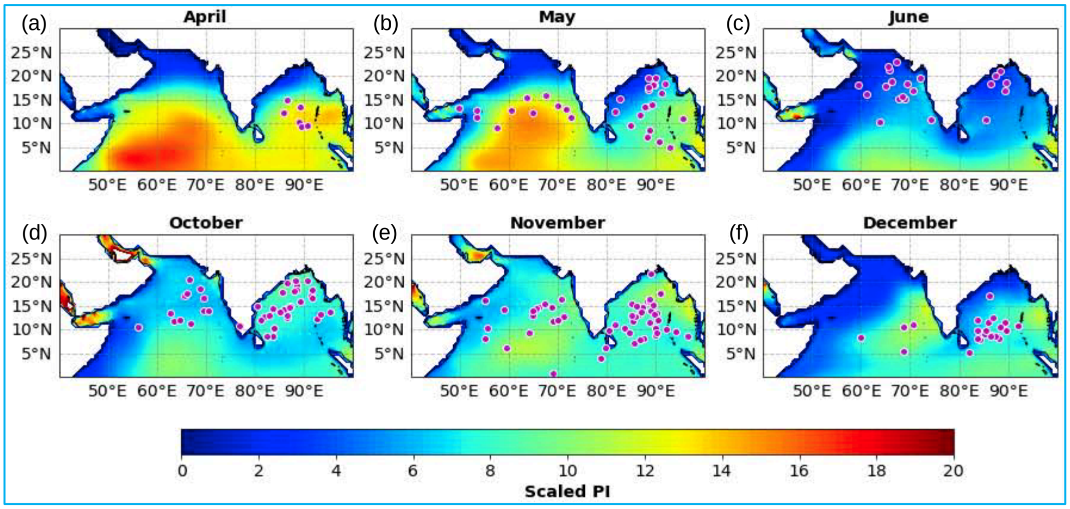

Figs. 13(a-f). TCGI-scaled climatological potential intensity (PI) values for different months. Top (bottom) row shows months of the pre-monsoon (post-monsoon) seasons. TC genesis locations given as magenta dots

months, while the shear is similar between the sub-basins. Only the humidity clearly favors the BOB over the AS consistently in all months shown.

3.5. *Role of humidity and shear in the monsoon season vs. the TC seasons*

While we conclude that humidity is more important than shear in keeping TC activity in the AS suppressed compared to that in the BoB, there is no doubt that shear controls the structure of the annual cycle in both basins. The very strong shear associated with the monsoon makes TC genesis virtually impossible in the entire NIO during the peak monsoon months of July, August and September, even though relative humidity (and all other environmental variables relevant to TC genesis) are favorable. While we focus on the pre-and post-monsoon TC seasons, analyses similar to those shown in Figs. 8(a-f) and 9(a-f), but for the entire seasonal cycle (not shown), confirm this. The impression we have from Figs. 8(a-f) and 9(a-f), in fact, is one in which NIO TCs occur in the windows in space and time when moisture is high enough but the strong monsoon shear is not present. In the AS, these windows are narrower due to its greater dryness compared to the BoB.

4. Conclusions

This study asks what environmental factors cause the Arabian Sea (AS) to experience fewer tropical cyclones (TCs) than the Bay of Bengal. We addressed this by analyzing environmental variables that are understood exert some control over TC genesis and quantifying the relative importance of those variables using a tropical cyclone genesis index (TCGI). Our primary results and conclusions are as follows:

(*i*) The TCGI predicts an overall rate of TC frequency in the NIO that is lower than that observed by approximately a factor of two. It is somewhat more successful in predicting the AS-BoB relative difference, however: the index reproduces the difference in the annual mean frequency with an error of 33%, though the errors are greater for the pre-and post-monsoons separately. Based on this partial success, we proceeded to analyze the relative contributions of the individual factors in the index.

(*ii*) Histograms of the individual monthly environmental variables in the months and locations of TC genesis show significant differences between the BoB and AS in vertical shear, column relative humidity and, to a lesser extent, potential intensity.

(*iii*) Further inspection of the spatial and seasonal structure of the climatological vertical shear, column relative humidity and potential intensity fields leads us to the conclusion that humidity is the most important factor that differentiates the AS from the BoB. Lower humidity in the AS during the pre-and post-monsoon seasons keeps TC activity there lower relative to the BoB. Potential intensity is similar between the sub-basins and may even slightly favour the AS over the BOB. And although vertical shear controls the seasonal cycle of TC activity in the entire NIO (suppressing TCs entirely during the peak monsoon months), shear differences between the AS & BoB are considerably smaller than humidity differences when the two are weighted by their importance to TC frequency, as measured by the TCGI.

Acknowledgments

AHS acknowledges support from the Monsoon Mission under India's Ministry of Earth Sciences. SJC acknowledges partial support from NOAA MAPP grants NA16OAR4310079 and NA18OAR4310277. We also acknowledge the Vetlesen Foundation for their generous and sustained support of climate science at the Lamont-Doherty Earth Observatory. The authors would like to thank Helena Rios, who performed preliminary analysis for this project during her summer internship in the Summer of 2018. The contents and views expressed in this research paper are the views of the authors and do not necessarily reflect the views of their organizations.

References

Baburaj, P., Abhilash, S., Mohankumar, K. and Sahai, A., 2020, "On the epochal variability in the frequency of cyclones during the pre-onset and onset phases of the monsoon over the north Indian ocean", *Advances in Atmospheric Sciences*, **37**, 634-651.

Balaji, M., Chakraborty, A. and Mandal, M., 2018, "Changes in tropical cyclone activity in north Indian ocean during satellite era (1981-2014)", *International Journal of Climatology*, **38**, 2819-2837.

Bell, S. S., Chand, S. S., Tory, K. J., Ye, H. and Turville, C., 2020, "North Indian Ocean tropical cyclone activity in CMIP5 experiments : Future projections using a model-independent detection and tracking scheme", *International Journal of Climatology*, doi:10.1002/joc.6594.

Bister, M. and Emanuel, K. A., 1998, "Dissipative heating and hurricane intensity", *Meteorology and Atmospheric Physics*, **65**, 233-240.

Bister, M. and Emanuel, K. A., 2002, "Low frequency variability of tropical cyclone potential intensity, part i, interannual to interdecadal variability", *Journal of Geophysical Research*, **107**, D24, 4801.doi:10.1029/2001JD000776.

Bretherton, C. S., Peters, M. E. and Back, L. E., 2004, "Relationships between water vapour path and precipitation over the tropical oceans", *Journal of Climate*, **17**, 1517-1528.

Camargo, S. J., Tippett, M. K., Sobel, A. H., Vecchi, G. A. and Zhao, M., 2014, "Testing the performance of tropical cyclone genesis indices in future climates using the HIRAM model", *J. Climate*, **27**, 9171-9196.

Chu, J. H., Sampson, C. R., Levine, A. S. and Fukada, E., 2002, "The Joint Typhoon Warning center tropical cyclone best-tracks, 1945-2000, *Tech. Rep.*, NRL/MR/7540-02-16, p22, Naval Research Laboratory.

Dee, D. P., Uppala, S. M., Simmons, A. J., Berrisford, P., Poli, P., Kobayashi, S., Andrae, U., Balmaseda, M. A., Balsamo, G., Bauer, P., Bechtold, P., Beljaars, A. C. M., van de Berg, L., Bidlot, J., Bormann, N., Delsol, C., Dragani, R., Fuentes, M., Geer, A. J., Haimberger, L., Healy, S. B., Hersbach, H., Hólm, E. V., Isaksen, L., Kållberg, P., Köhler, M., Matricardi, M., McNally, A. P., Monge Sanz, B. M., Morcrette, J. J., Park, B. K., Peubey, C., Rosnay, P. De, Tavolato, C., Thépaut, J. N., Vitart, F., 2011, "The ERA-Interim reanalysis : Configuration and performance of the data assimilation system", *Quarterly Journal of the Royal Meteorological Society*, **137**, 553-597.

Emanuel, K. A., 1988, "The maximum intensity of hurricanes", *Journal of the Atmospheric Sciences*, **45**, 1143-1155.

Evan, A. T. and Camargo, S. J., 2011, "A climatology of arabian sea cyclonic storms", *Journal of Climate*, **24**, 140-158.

Gray, W. M., 1968, "Global view of the origin of tropical disturbances and storms", *Monthly Weather Review*, **96**, 669-700.

IMD, 2011, "Cyclone eAtlas : Tracks of cyclones and depressions over the North Indian Ocean (from 1891 onwards)", Tech. Rep. Electronic version 2.0/2011, Cyclone Warning & Research Centre, IMD, Chennai, India.

Kossin, J. P., Knapp, K. R., Olander, T. L. and Velden, C. S., 2020, "Global increase in major tropical cyclone exceedance probability over the past four decades", *Proceedings of the National Academy of Sciences*, **117**, 11975-11980.

Li, Z., K. L. Weidong Y., Wang, H. and Liu, L. 2019, "Environmental conditions modulating tropical cyclone formation over the Bay of Bengal during the pre-monsoon transition period", *Journal of Climate*, **32**, 4387-4394.

Mann, H. B. and Whitney, D. R., 1947, "On a test of whether one of two random variables is stochastically larger than the other", *The Annals of Mathematical Statistics*, **18**, 50-60.

Murakami, H. and Sugi, M., 2012, "Future changes in tropical cyclone activity in the North Indian Ocean projected by high-resolution MRI-AGCMs", *Climate Dynamics*, **40**, 1949-1968.

Murakami, H., Vecchi, G. A. and Underwood, S., 2017, "Increasing frequency of extremely severe cyclones over the Arabian Sea", *Nature Climate Change*, **7**, 885-889.

Ng, E. K. W. and Chan, J. C. L., 2012, "Interannual variations of tropical cyclone activity over the north Indian ocean", *International Journal of Climatology*, **32**, 819-830.

Sahoo, B. and Bhaskaran, P. K., 2016, "Assessment on historical cyclone tracks in the Bay of Bengal, east coast of India", *International Journal of Climatology*, **36**, 95-109.

Sattar, A. M. and Cheung, K. K., 2019, "Comparison between the active tropical cyclone seasons over the Arabian sea and Bay of Bengal", *International Journal of Climatology*, **39**, 5482-5502.

Schreck, C. J., Knapp, K. K. and Kossin, J. P., 2014, "The impact of best track discrepancies on global tropical cyclone climatologies using IBTrACS", *Monthly Weather Review*, **142**, 3881-3899.

Singh, K., Panda, J. and Mohapatra, M., 2020, "Robustness of best track data and associated cyclone activity over the north Indian ocean region during and prior to satellite era", *Journal of Earth System Science*, **129**, p84.

Singh, K., Panda, J., Osuri, K. K. and Vissa, N. K., 2016, "Progress in Tropical Cyclone Predictability and Present Status in the North Indian Ocean Region", *Tropical Cyclone Dynamics, Prediction and Detection*, A. R. Lupo, Ed., Intech Open, Rijeka, Chap. 9. doi:10.5772/64333, URL https://doi.org/10.5772/64333.

Singh, K., Panda, J., Sahoo, M. and Mohapatra, M., 2019, "Variability in tropical cyclone climatology over North Indian Ocean during the period 1891 to 2015", *Asia-Pacific Journal of Atmospheric Sciences*, **55**, 269-287.

Tippett, M. K., Camargo, S. J. and Sobel, A. H., 2011, "A poisson regression index for tropical cyclone genesis and the role of large-scale vorticity in genesis", *Journal of Climate*, **24**, 2335-2357.

Vishnu, S., Sanjay, J. and Krishnan, R., 2019, "Assessment of climatological tropical cyclone activity over the North Indian Ocean in the CORDEX-South Asia regional climate models", *Climate Dynamics*, **53**, 5101-5118.